

## Chaotic spin correlations in frustrated Ising hierarchical lattices

Neşe Aral<sup>1</sup> and A. Nihat Berker<sup>1,2,3</sup>

<sup>1</sup>College of Arts and Sciences, Koç University, Sarıyer, 34450 Istanbul, Turkey

<sup>2</sup>Department of Physics, Massachusetts Institute of Technology, Cambridge, Massachusetts 02139, USA

<sup>3</sup>Feza Gürsey Research Institute, TÜBİTAK - Bosphorus University, Çengelköy, 34684 Istanbul, Turkey

(Received 15 December 2008; published 23 January 2009)

Spin-spin correlations are calculated in frustrated hierarchical Ising models that exhibit chaotic renormalization-group behavior. The spin-spin correlations, as a function of distance, behave chaotically. The far correlations, but not the near correlations, are sensitive to small changes in temperature or frustration, with temperature changes having a larger effect. On the other hand, the calculated free energy, internal energy, and entropy are smooth functions of temperature. The recursion-matrix calculation of thermodynamic densities in a chaotic band is demonstrated. The leading Lyapunov exponents are calculated as a function of frustration.

DOI: 10.1103/PhysRevB.79.014434

PACS number(s): 75.10.Nr, 05.10.Cc, 05.45.Gg, 64.60.aq

It was shown some time ago that frustrated Ising spin magnetic systems exhibit chaotic behavior of the interaction constants under renormalization-group transformations, which readily leads to the description of a spin-glass phase.<sup>1</sup> This chaotic rescaling behavior was originally demonstrated in frustrated but nonrandom systems. It was subsequently shown that the same chaotic rescaling behavior occurs in quenched random spin glasses.<sup>2</sup> Chaotic rescaling behavior has now been established as the signature of a spin-glass phase.<sup>3–12</sup> Although the chaotic behavior of the interaction constants was demonstrated in frustrated systems, the behavior of spin-spin correlation functions and the instabilities to initial conditions had not been calculated to date. This study presents such results, yielding both smooth and unsmooth behaviors, as seen below. In this process, the recursion-matrix calculation of thermodynamic densities in a chaotic band is demonstrated.

Hierarchical models are exactly soluble models that exhibit nontrivial cooperative and phase-transition behaviors<sup>13–15</sup> and have therefore become the testing grounds for a large variety of phenomena, as also seen in recent works.<sup>16–27</sup> The hierarchical models in which the chaotic rescaling behavior of the interaction constants under frustration was seen<sup>1</sup> are defined in Fig. 1. The two units [Figs. 1(a) and 1(b)] assembled in the construction of these lattices *a priori* represent the generically distinct local effects of frustration occurring in spin-glass systems on conventional lattices. In Fig. 1(a), correlation at the small scale (vertical bonds) inhibits at low temperatures the propagation of correlation at the larger scale (horizontally across the unit), namely, causing a *disordering by ordering*. In Fig. 1(b), competition between paths of different lengths weakens but does not eliminate the propagation of correlation across the unit. These two generic effects are incorporated into the hierarchical lattices of Fig. 1. No other such generic effects occur in spin glasses.

**Renormalization-group transformation.** Hierarchical lattices are constructed by the repeated self-embedding of graphs.<sup>13–15</sup> Their solution, by renormalization-group theory, consists of the reverse procedure. The number of bonds of the imbedding graph gives the volume rescaling factor,  $b^d = (4+p)p_a + (m_1+m_2)p_b$ , in the current case, and the shortest path length across the imbedding graph gives the length rescaling factor,  $b=2$  here, leading here to a dimensionality  $d$

that is greater than 2. Each straight-line segment in Fig. 1 corresponds to an interaction  $-\beta H_{ij} = K\sigma_i\sigma_j + G$  with  $K \geq 0$  between Ising spins  $\sigma_i = \pm 1$  at vertices  $i$ . Frustration is introduced by the wiggly bonds. The additive constant  $G$  is generated by the renormalization-group transformation and enters the calculation of the thermodynamic functions and correlations of the original unrenormalized system.<sup>28</sup> The renormalization-group transformation consists in summing, in the partition function, over the internal spins of the innermost imbedding graphs, which are thereby replaced by a renormalized bond with

$$K' = p_a \tanh^{-1} \tilde{t}_a + p_b (\tanh^{-1} t^{m_1} - \tanh^{-1} t^{m_2}),$$

where

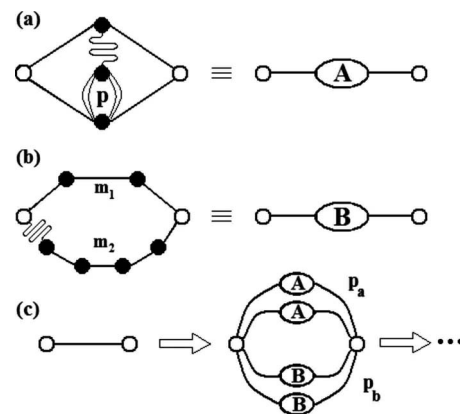


FIG. 1. The family of hierarchical models from Ref. 1. In unit (a), there are  $p$  cross bonds. In unit (b), two paths, consisting of  $m_1$  and  $m_2 > m_1$  bonds in series, are in parallel. In (c), the final graph of the model is assembled with  $p_a$  and  $p_b$  of each unit in parallel. Each wiggly bond, representing an infinite antiferromagnetic coupling, has the effect of reversing the sign of an adjoining bond.

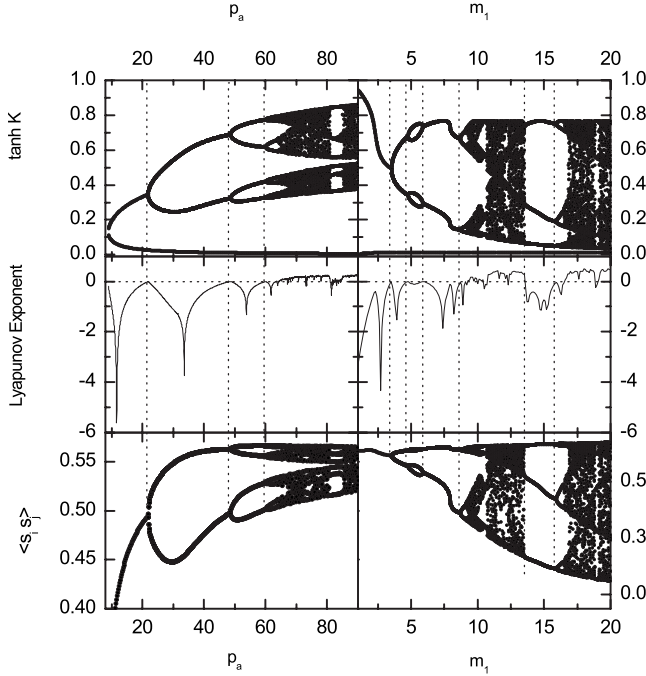


FIG. 2. Renormalization-group flow topologies, Lyapunov exponents, and spin-spin correlations, as Hamiltonian parameters are scanned. In both examples,  $p=5$ ,  $p_b=2$ , and  $m_2=m_1+5$ . In the upper panels, the lower curve, visible on the left, is a line of unstable fixed points, giving the second-order phase transition between the paramagnetic (below) and ordered (above) phases. In the ordered phase, only fixed points, limit cycles, and chaotic bands that are stable (attractive) are shown. In the lower panels, the spin-spin correlation function  $\langle s_i s_j \rangle$  for spins separated by a distance  $2^n$  are given for consecutive  $n$  at each value of the Hamiltonian parameters. It is shown in the text that the Lyapunov exponents, middle panels, apply to both upper and lower panels. Left panels: scanning  $p_a$ , which increases the disordering by ordering effect, at  $m_1=5$ . Right panels: scanning  $m_1$ , which increases the ground-state entropy of per first renormalized bond at  $p_a=50$ .

$$\tilde{t}_a = 2t^2(1 - \tilde{t}) / (1 + t^4 - 2t^2\tilde{t}),$$

$$G' = b^d G + [2p_a + (m_1 + m_2 - 2)p_b] \ln 2 - p_a p K + \frac{p_a}{2} \ln \frac{(1+t^2)^2 - 4t^2\tilde{t}}{(1-t^2)^2(1-\tilde{t})^2} + \frac{p_b}{2} \ln \frac{(1-t^{2m_1})(1-t^{2m_2})}{(1-t^2)^{m_1+m_2}}, \quad (1)$$

with  $t = \tanh K$  and  $\tilde{t} = \tanh(pK)$ .

**Results: Self-similar chaotic bands.** When this family of models is scanned as a function of  $p_a$  or  $m_1$ , respectively increasing the *disordering by ordering* effect or the ground-state entropy per first renormalized bond, the chaotic behavior of the renormalization group is entered, in the low-temperature phase, via the series of period-doubling bifurcations, with the Feigenbaum exponent of 4.669,<sup>1</sup> as shown in Fig. 2. An example of the chaotic bands of the interaction constant is shown in Fig. 3(a). Discovery of these chaotic bands immediately led to a spin-glass interpretation: under repeated scale changes, the entire band is visited by

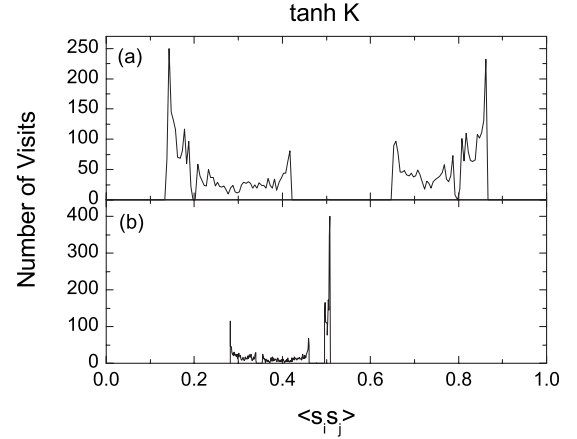


FIG. 3. (a) Number of visits per interaction interval  $\Delta t=0.005$  for 5000 chaotic iterations in the trajectory starting at  $t^{(0)}=0.5$  and for  $p=4$ ,  $p_a=40$ ,  $p_b=1$ ,  $m_1=4.7$ , and  $m_2=m_1+1$ . (b) Number of visits per correlation interval  $\Delta \langle s_i s_j \rangle=0.005$  for the trajectory in (a).

the effective coupling of the length scales that are reached after each renormalization-group transformation. This chaotic sequence of hopping visits stretches from the strong-coupling to the weak-coupling edges of the band. This signifies that as the system is viewed at successive length scales, strong and weak correlations are encountered in a frozen but chaotic sequence, meaning a spin-glass phase. This interpretation had not been followed by an actual calculation of these spin-spin correlations, which is done in the current study.

Also shown in Fig. 2 are the leading Lyapunov exponents ( $\lambda$ ) used to describe the behavior of a dynamical system that starts at  $x_0$  and evolves for  $n$  iterations,  $x_{i+1}=f(x_i)$ ,

$$\lambda = \lim_{n \rightarrow \infty} \frac{1}{n} \sum_{k=0}^{n-1} \ln \left| \frac{dx_{k+1}}{dx_k} \right|. \quad (2)$$

The iteration function  $f$  may depend on different parameters, as our iteration function  $K'(K)$  depends on  $m_1$  and  $p_a$ . Such an iterated map function has a chaotic trajectory for a par-

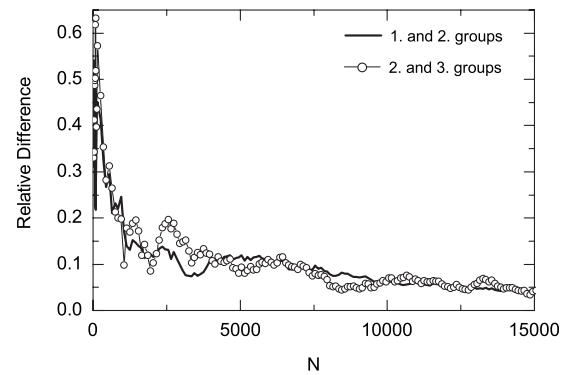


FIG. 4. Overlaps between consecutive groups of  $N$  iterations for the trajectory in Fig. 3(a). The relative difference  $\frac{1}{200} \sum_{i=1}^{200} |\Delta n_i| / \bar{n}_i$ , between two consecutive groups, in the number of visits  $n_i$  to each of the 200 interaction intervals  $i$  is shown as a function of group size  $N$ .

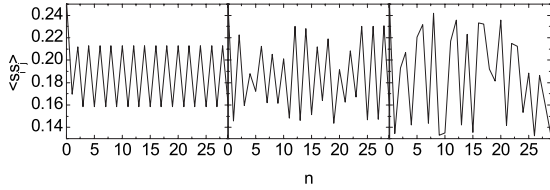


FIG. 5. The spin-spin correlation function  $\langle s_i s_j \rangle$  for spins separated by a distance  $2^n$  for  $K=2.5$ ,  $p=4$ ,  $p_a=40$ ,  $p_b=1$ ,  $m_1=3.7, 4.7, 5.7$ , and  $m_2=m_1+1$ .

ticular parameter value if the Lyapunov exponent is positive. Conversely, a negative  $\lambda$  indicates eventual attraction to a fixed point or a limit cycle. A bifurcation point, where a period doubling occurs, is identified with  $\lambda$  being zero.<sup>29</sup> Furthermore,

$$\frac{d\langle s_i s_j \rangle_{k+1}}{d\langle s_i s_j \rangle_k} = \frac{d\langle s_i s_j \rangle_{k+1}}{d \tanh(K_{k+1})} \frac{d \tanh(K_{k+1})}{d \tanh(K_k)} \frac{d \tanh(K_k)}{d\langle s_i s_j \rangle_k}, \quad (3)$$

so that the first and last factors from Eq. (3) cancel out in the successive terms in Eq. (2). Thus, the interaction constants and the spin-spin correlations have the same Lyapunov exponents.

An important characteristic of the chaotic bands is that they are self-similar: after the transient behavior of a number of renormalization-group transformations, the profile of the chaotic band formed by each successive group of  $N$  renormalization-group calculations becomes identical in the limit of large  $N$ . The overlaps between such successively formed bands are shown as a function of  $N$  in Fig. 4. Physically, this signifies that a geometrically coarse-grained spin-glass phase is self-similar. This property of the chaotic bands is important in the calculation of the correlation functions.

*Results: Calculation of the correlation functions.* The recursion relation for the densities is<sup>28</sup>

$$[1, \langle s_i s_j \rangle] = b^{-d} [1, \langle s_i s_j \rangle'] \begin{pmatrix} b^d & \frac{\partial G'}{\partial K} \\ 0 & \frac{\partial K'}{\partial K} \end{pmatrix}. \quad (4)$$

In an ordinary renormalization-group analysis, this density recursion relation is iterated,

$$[1, \langle s_i s_j \rangle] = b^{-dn} [1, \langle s_i s_j \rangle^{(n)}] T^{(n)} T^{(n-1)} \dots T^{(1)}, \quad (5)$$

until the  $(n)$ th renormalized system is as close as one desires to a sink fixed point, and the renormalized densities  $[1, \langle s_i s_j \rangle^{(n)}]$  are inserted as the left eigenvector of  $T^{(n)}$  with eigenvalue  $b^d$ .<sup>28</sup> In the current calculation, this cannot be done since the renormalization-group trajectory does not approach a sink fixed point but chaotically wanders inside a band. On the other hand, in this chaotic-band sink, we obtain the limiting behavior due to the self-similarity property of the chaotic band,

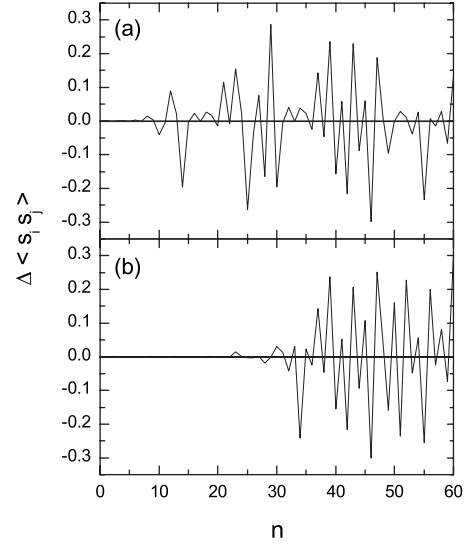


FIG. 6. Deviations, for small temperature or frustration change, in the spin-spin correlation function  $\langle s_i s_j \rangle$  for spins separated by a distance  $2^n$  and for  $K=0.8$ ,  $p=4$ ,  $p_a=40$ ,  $p_b=1$ ,  $m_1=8$ , and  $m_2=m_1+1$ . In (a) and (b), between the two trajectories,  $\Delta K=0.001$  and  $\Delta p_a=0.001$ , respectively.

$$b^{-dn} T^{(n)} T^{(n-1)} \dots T^{(1)} \approx \begin{pmatrix} 1 & X \\ 0 & 0 \end{pmatrix}, \quad (6)$$

so that  $X = \langle s_i s_j \rangle$  and this result is independent of the chaotic-band terminus  $\langle s_i s_j \rangle^{(n)}$ . The disappearance of the lower diagonal reflects  $\partial K' / \partial K < b^d$ , itself due to sequential noninfinite

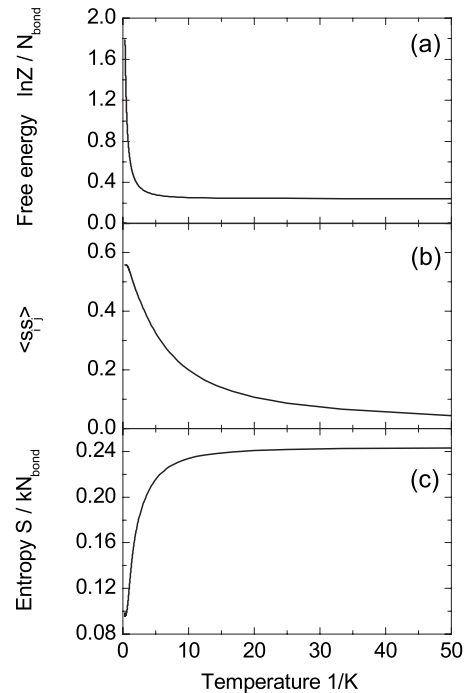


FIG. 7. For model parameters  $p=4$ ,  $p_a=10$ ,  $p_b=1$ ,  $m_1=7$ , and  $m_2=m_1+1$ , (a) free energy per bond,  $F = \ln Z / N_{\text{bond}}$ , (b) internal energy,  $U = \langle s_i s_j \rangle$ , (c) entropy per bond,  $S = \ln Z / N_{\text{bond}} - K \langle s_i s_j \rangle$ , versus temperature  $K^{-1}$ .

bonds and frustration in the chaotic-band sink. Alternately,  $\langle s_i s_j \rangle$  can be calculated from numerical differentiation of the free energy obtained from the renormalization of the additive constant  $G$ .

The calculated spin-spin correlations as a function of spin separation are shown in Fig. 5. It is seen that the spin-spin correlations behave chaotically, for all distances, between strong and weak correlations, numerically justifying the spin-glass phase interpretation. Thus, spin-spin correlations also span chaotic bands, as illustrated in Fig. 2, lower panels, and Fig. 3(b).

*Results: Unsmooth and smooth behaviors.* Figure 6 shows the behavior, at all distances, of the spin-spin correlations under small changes in temperature or frustration. It is seen that the near correlations are unaffected, whereas the far correlations are strongly affected, namely, randomly changed, with temperature changes having a larger such effect.

Finally, the free energy, calculated from summing the ad-

ditive constants generated by the successive renormalization-group transformations, the internal energy, calculated from the nearest-neighbor spin-spin correlation, and the entropy are shown in Figs. 7(a)–7(c) as a function of temperature. They exhibit smooth behaviors. Zero-temperature entropy,<sup>30</sup> due to frustration, is seen.

In closing, we note that other forms of chaotic behavior, namely, as a function of system size<sup>31</sup> or as the chaos of near-neighbor correlations in the zero-temperature limit for appropriately chosen interactions,<sup>32</sup> intriguingly occur in spin-glass systems. In contrast to our current results, the renormalization of correlations in a strange nonchaotic attractor is given in Ref. 33.

This research was supported by the Scientific and Technological Research Council of Turkey (TÜBİTAK) and by the Academy of Sciences of Turkey.

- 
- <sup>1</sup>S. R. McKay, A. N. Berker, and S. Kirkpatrick, Phys. Rev. Lett. **48**, 767 (1982).  
<sup>2</sup>E. J. Hartford and S. R. McKay, J. Appl. Phys. **70**, 6068 (1991).  
<sup>3</sup>F. Krzakala and J. P. Bouchaud, Europhys. Lett. **72**, 472 (2005).  
<sup>4</sup>M. Sasaki, K. Hukushima, H. Yoshino, and H. Takayama, Phys. Rev. Lett. **95**, 267203 (2005).  
<sup>5</sup>J. Lukic, E. Marinari, O. C. Martin, and S. Sabatini, J. Stat. Mech.: Theory Exp. (2006) L10001.  
<sup>6</sup>P. Le Doussal, Phys. Rev. Lett. **96**, 235702 (2006).  
<sup>7</sup>T. Rizzo and H. Yoshino, Phys. Rev. B **73**, 064416 (2006).  
<sup>8</sup>H. G. Katzgraber and F. Krzakala, Phys. Rev. Lett. **98**, 017201 (2007).  
<sup>9</sup>H. Yoshino and T. Rizzo, Phys. Rev. B **77**, 104429 (2008).  
<sup>10</sup>T. Aspelmeier, Phys. Rev. Lett. **100**, 117205 (2008).  
<sup>11</sup>T. Aspelmeier, J. Phys. A **41**, 205005 (2008).  
<sup>12</sup>T. Mora and L. Zdeborova, J. Stat. Phys. **131**, 1121 (2008).  
<sup>13</sup>A. N. Berker and S. Ostlund, J. Phys. C **12**, 4961 (1979).  
<sup>14</sup>R. B. Griffiths and M. Kaufman, Phys. Rev. B **26**, 5022 (1982).  
<sup>15</sup>M. Kaufman and R. B. Griffiths, Phys. Rev. B **30**, 244 (1984).  
<sup>16</sup>A. Erbaş, A. Tuncer, B. Yücesoy, and A. N. Berker, Phys. Rev. E **72**, 026129 (2005).  
<sup>17</sup>M. Hinczewski and A. N. Berker, Phys. Rev. E **73**, 066126 (2006).  
<sup>18</sup>M. Hinczewski, Phys. Rev. E **75**, 061104 (2007).  
<sup>19</sup>Z. Z. Zhang, Z. G. Zhou, and L. C. Chen, Eur. Phys. J. B **58**, 337 (2007).  
<sup>20</sup>E. Khajeh, S. N. Dorogovtsev, and J. F. F. Mendes, Phys. Rev. E **75**, 041112 (2007).  
<sup>21</sup>H. D. Rozenfeld and D. ben-Avraham, Phys. Rev. E **75**, 061102 (2007).  
<sup>22</sup>M. Kaufman and H. T. Diep, J. Phys.: Condens. Matter **20**, 075222 (2008).  
<sup>23</sup>F. A. P. Polho, F. A. da Costa, and C. G. Bezerra, Physica A **387**, 1538 (2008).  
<sup>24</sup>N. S. Branco, J. R. de Sousa, and A. Ghosh, Phys. Rev. E **77**, 031129 (2008).  
<sup>25</sup>T. Jorg and F. Ricci-Tersenghi, Phys. Rev. Lett. **100**, 177203 (2008).  
<sup>26</sup>S. Boettcher, B. Goncalves, and J. Azaret, J. Phys. A **41**, 335003 (2008).  
<sup>27</sup>C. Monthus and T. Garel, J. Phys. A **41**, 375005 (2008).  
<sup>28</sup>S. R. McKay and A. N. Berker, Phys. Rev. B **29**, 1315 (1984).  
<sup>29</sup>R. C. Hilborn, *Chaos and Nonlinear Dynamics*, 2nd ed. (Oxford University Press, New York, 2003).  
<sup>30</sup>A. N. Berker and L. P. Kadanoff, J. Phys. A **13**, L259 (1980); **13**, 3786 (1980).  
<sup>31</sup>C. M. Newman and D. L. Stein, J. Phys.: Condens. Matter **15**, R1319 (2003).  
<sup>32</sup>A. C. D. van Enter and W. M. Ruszel, J. Stat. Phys. **127**, 567 (2007).  
<sup>33</sup>U. Feudel, A. Pikovsky, and A. Politi, J. Phys. A **29**, 5297 (1996).